2005 ANNUAL REPORT

Kinematic Rupture Model Generator

Robert W. Graves, URS Group, Inc.

Objective

There are several ongoing efforts within SCEC that involve the use of ground motion simulations for scenario earthquakes. These include the NSF Project on Implementation Interface (NGA-H, structural response simulations) and Pathway II components of CME. Additionally, developments are underway within the Seismic Hazard Analysis focus group to implement time history generation capabilities (e.g., CyberShake). A key component that these projects all depend upon is the ability to generate physically plausible earthquake rupture models, and to disseminate these models in an efficient, reliable and self-consistent manner. The work presented here takes the first step in addressing this need by developing a computation module to specify and generate kinematic rupture models for use in numerical earthquake simulations. The computational module is built using pre-existing models of the earthquake source (e.g., pseudo-dynamic, K^{-2} wavenumber decay, etc…). In the initial implementation, we have employed simple rules to compute rupture initiation time based on scaling of the local shear wave velocity. The slip velocity function is a simplified Kostrov-like pulse, with the rise time given by a magnitude scaling relation. However, the module is not restricted to accept only these parameterizations, but is instead constructed to allow alternative parameterizations to be added in a straightforward manner. One of the most important features of the module is the use of a Standard Rupture Format (SRF) for the specification of kinematic rupture parameters. This will help ensure consistent and accurate representation of source rupture models and allow the exchange of information between various research groups to occur in a more seamless manner.

General Procedure

In the kinematic description, the fault rupture is represented as a distribution of point sources spread across the fault surface. The strength of each point source is proportional to the local fault displacement and the initiation time is lagged to represent rupture propagation from the prescribed hypocenter. The displacement time history at each point is given by a prescribed slip function. While it is recognized that the kinematic representation provides no guarantee that the resulting rupture model is physically plausible, its simplicity offers an attractive alternative while more complex dynamic rupture generators are being developed.

Given a general description of the fault surface, including length, width, depth to top, and average strike, dip and rake, the rupture generation process consists of the following steps (described in more detail in the adjacent panels):

Step 1: Determine M_w using Area *vs*. M_w relation.
Step 2: Generate slip distribution.
Step 3: Specify hypocenter and rupture times.
Step 4: Specify slip function.

Step 1: Area vs. Magnitude Relation

The magnitude (or moment) is required for two purposes. First, several of the kinematic parameters (e.g., corner wavenumber, rise time) are related to the magnitude through scaling relations, and second, the final slip distribution must be scaled to give the target moment. There are several Area vs. M_w relations currently available (e.g. Wells and Coppersmith, 1994; Somerville *et al*. 1999; Ellsworth, 2002; Hanks and Bakun, 2002). In practice, any of these can be sued with the rupture generation procedure. However, differences in these relations can have a significant impact on the resulting fault slip amounts, and hence, on the ground motion levels predicted from these rupture models using waveform simulations.

For demonstration purposes, we have used the relation of Somerville et al. (1999) in generating the slip distributions shown in this report,

$$M_w = 3.98 + \log_{10} (Area)$$

Where *Area* is given in km^2.

Step 2: Generate Slip Distribution

The slip distribution is generated in the wavenumber domain by constraining the amplitude spectrum to fit a prescribed decay model. Theoretical studies suggest that the amplitude spectrum fall of as K^{-2} (e.g., Andrews, 1980; Herrero and Bernard, 1994). Empirical analyses of slip distributions of past earthquakes also suggest a similar model (e.g., Somerville et al., 1999; Mai and Beroza, 2002). While the specific form of these models may differ (e.g., butterworth-type, von-Karman, etc.), the key parameter controlling the fall-off in all models is the correlation length or corner wavenumber. This parameter determines the characteristic size of the large slip patches (asperities). Mai and Beroza (2002) discuss this issue in more detail. In all of these models, the phase of the spectrum is random.

In the examples shown here, we have used the Somerville et al. (1999) spectral filter

$$A(k) = F(1+K_o^4)^{-1/2}$$

where $K_o^2 = (k_x^2 x_L^2 + k_y^2 y_L^2)$ is the normalized wavenumber, x_L and y_L are the correlation lengths given by

$$\log_{10} x_L = \log_{10} y_L = 0.5 M_w – 2$$

and F is a scaling factor given to the correct moment.

In practice, we start with a spatially uniform slip distribution, transform into the wavenumber domain, and then apply the amplitude filter with random phase. No filtering is applied for wavenumbers below $k = 4 dk$, thus preserving the long wavelength features of the initial slip distribution. This tends to prevent regions of negative slip from occurring. Hermitian symmetry ensures a purely real spatial slip function. After transforming back to the spatial domain, the edges of the slip distribution are tapered and any negative slip values are truncated to zero. For surface rupturing events, no taper is applied at the top (see M_w 7.5 example below). All transforms are done using an exact length Fourier transform thus alleviating the need for padding.

Figure 1 shows 5 slip realizations for M_w 6.5 and 7.5 events. Different realizations are generated by changing the random number seed for the phasing. Figure 2 shows the wavenumber spectral ratio for the five slip models at each M_w, as well as their average. The spectral ratio is defined as the computed amplitude spectrum divided by the model spectrum. Individual slip realizations show some minor deviation from the model; however, on average the fit is quite good.

Step3: Specify Hypocenter and Rupture Times

The understanding of the parameters and forces that govern the initiation of rupture during large earthquakes is still very limited. Most ruptures appear to initiate on the deeper portions of faults (presumably where the strength is high), but the along strike location is currently very difficult to predict. In the kinematic approach, we constrain the hypocenter to be in the bottom ¼ of the fault plane. The along strike location can be random or prescribed. Currently, no attempt is made to correlate the hypocenter with the asperity distribution, although this could be added in future versions (e.g., Guatteri *et al*., 2004).

The rupture initiation time is given by

$$T_i = R / V_r - \delta t$$

Where R is the rupture path length from the hypocenter, V_r is the rupture velocity and is set at 80% of the local shear wave velocity.

δt is a timing perturbation that scales linearly with slip amplitude such that $\delta t = \delta t_o$ where the slip is at its maximum and $\delta t = 0$ where the slip is at the average slip value. We set $\delta t_o = 0.5$ sec. This scaling results in faster rupture across portions of the fault having large slip, consistent with some dynamic rupture models and as suggested by source inversions of past earthquakes (see Figure 3).

Step 4: Specify Slip Function

We use a slip velocity function that is constructed using two triangles as shown in Figure 4. This functional form is based on results of dynamic rupture simulations (e.g., Guaterri et al., 2003). We constrain the parameters of this function as follows:

$$T_r = 1.8 \times 10^{-9} M_o^{1/3}$$
$$T_p = 0.2\, T_r$$
$$h = 0.2\, A$$

where M_o is the seismic moment (dyne-cm), T_r is the rise time and A is normalized to give the desired final slip. The expression for T_r comes from the empirical analysis of Somerville *et al*. (1999). In general, T_r may vary across the fault; however, in practice we only allow a depth dependent scaling such that T_r increases by a factor of 2 between 0 and 5 km depth (Kagawa *et al*., 2001).

Implementation in CME

A software module for the kinematic rupture generator has been developed and implemented into the computational framework of the Community Modeling Environment. This module is currently being utilized to generate rupture models for use in the Cyber Shake project.

References

Andrews, D. J. (1980). Fault impedance and earthquake energy in the Fourier transform domain, *Bull. Seism. Soc. Am.*, **70**, 1683-1689.

Graves, R. W. and A. Pitarka (2004). Broadband time history simulation using a hybrid approach, *Proc. 13th World Conf. Earthquake Eng.*, Vancouver, Canada, paper no. 1098.

Guatteri, M., P. M. Mai, G. C. Beroza, and J. Boatwright (2003). Strong ground motion prediction from stochastic dynamic source models, *Bull. Seism. Soc. Am.*, **93**, 301-313.

Hartzell, S. H., P. Liu, and C. Mendoza (1996). The 1994 Northridge, California earthquake: Investigation of rupture velocity, rise time, and high frequency radiation, *J. Geophys. Res.*, **101**, 20,091-20,108.

Kagawa, T., K. Irikura, and P. Somerville (2001). A study on ground motion and fault rupture due to subsurface faults, *Eos. Trans. AGU*; **82**(47): Fall Meet. Suppl., Abstract S31C-06.

Mai, P. M. and G. C. Beroza (2002). A spatial random field model to characterize complexity in eartqhauke slip, *J. Geophys. Res.*, **107**, 2308-2326.

Somerville P, Irikura K, Graves R, Sawada S, Wald D, Abrahamson N, Iwasaki Y, Kagawa T, Smith N, Kowada A. (1999). Characterizing crustal earthquake slip models for the prediction of strong ground motion. *Seism. Res. Lett.*; **70**, 59-80.

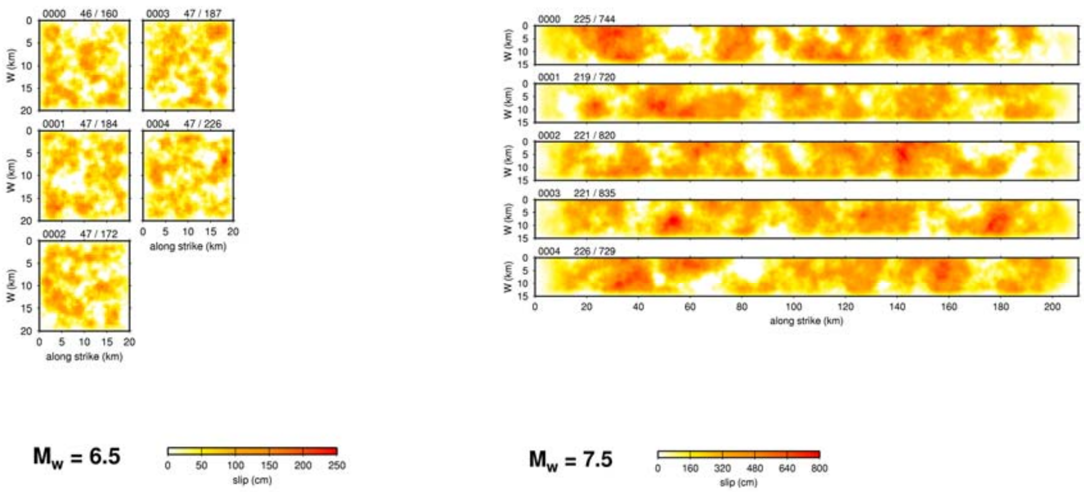

Figure 1: Slip distributions for Mw 6.5 (left) and Mw 7.5 (right) events. Phasing of asperities is random and final displacement is scaled to target moment using a prescribed 1D velocity structure.

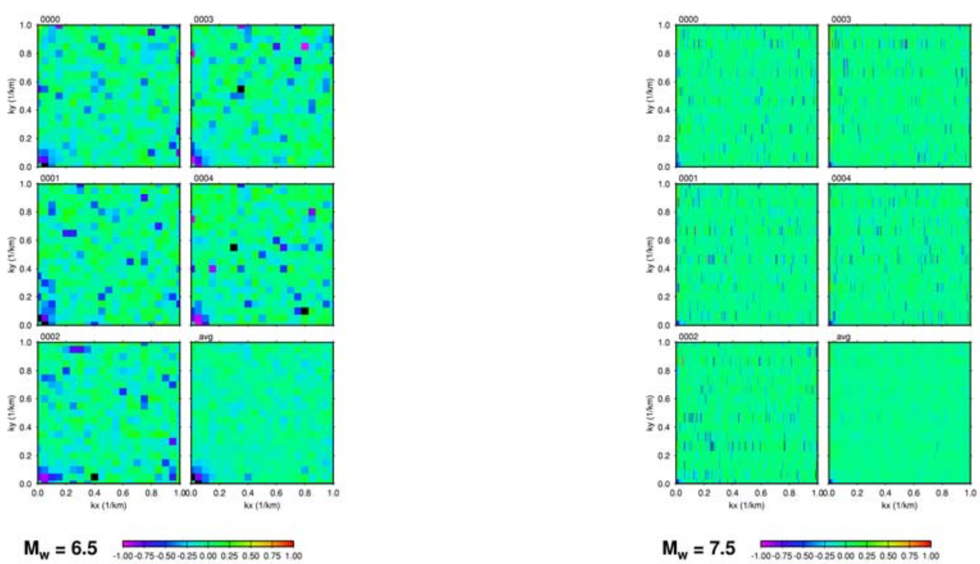

Figure 2: Ratio of the wavenumber spectra for the slip distributions shown in Figure 1 relative to the target amplitude spectrum. The bottom right panel for each magnitude shows the average of the five individual spectra.

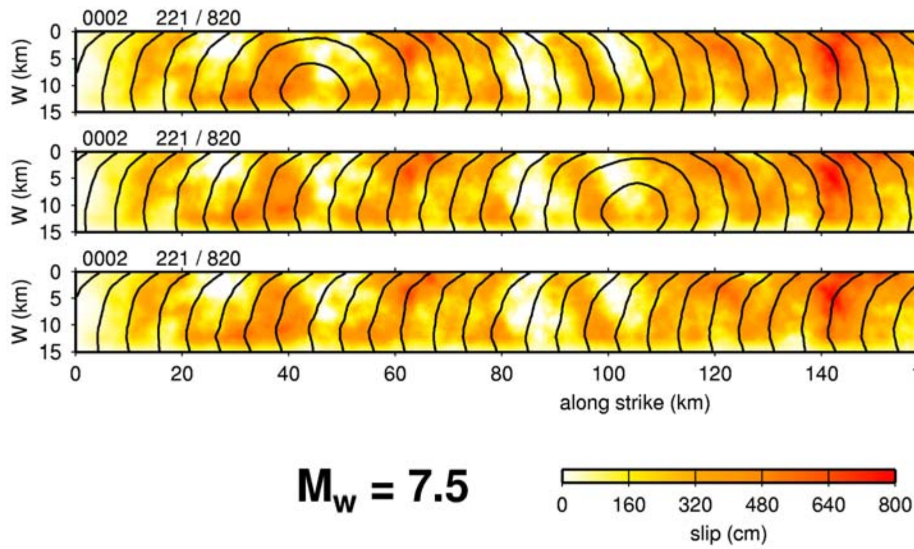

Figure 3: Rupture propagation contours (1 sec intervals) for 3 hypocenter locations for a given slip distribution of a Mw 7.5 event.

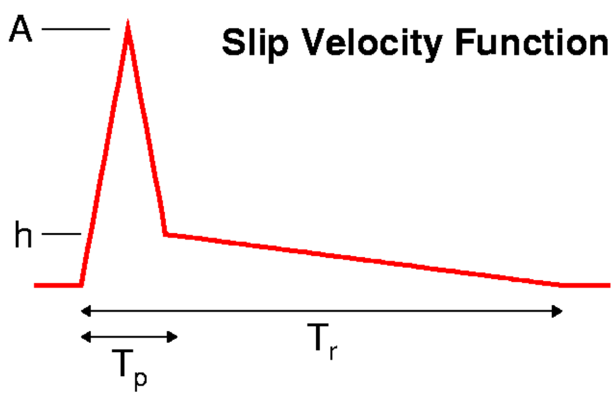

Figure 4: Schematic representation of the slip velocity function used in the rupture specification.